

# Optimal Stochastic Scheduling of Virtual Power Plant Considering NaS Battery Storage and Combined Heat and Power Units

MORTEZA NAZARI-HERIS<sup>1</sup>, SAJAD MADADI<sup>2</sup>, SAEED ABAPOUR<sup>3</sup>, AND BEHNAM MOHAMMADI-IVATLOO<sup>4</sup>

<sup>1,2,3,4</sup>Smart Energy Systems Laboratory, Faculty of Electrical and Computer Engineering, University of Tabriz, Tabriz, Iran.

\* Corresponding author:mnazari@tabrizu.ac.ir

Manuscript received 26 May, 2018; Revised 20 July, 2018, accepted 22 July, 2018. Paper no. JEMT- 1095.

The penetration level of distributed generations and renewable energy sources have been generally increased in power systems. However, such generation units with small capacities are not able to participate in electricity markets. Therefore, virtual power plant (VPP) concept is defined to integrate such power plants and cooperate them into power markets. A well-known type of distributed generation is combined heat and power (CHP) units, which has attracted significant efforts in recent years. In this paper, a VPP is modelled to obtain optimal participate into day-ahead market and response to local heat demand. The VPP includes wind power, two types of CHP units, NaS battery for electrical components and CHP units, heat storage, and boiler unit. Moreover, the stochastic model is accounted for scheduling of VPP to meet uncertainty of wind power units. The proposed stochastic model for the VPP is simulated, and the simulation results are reported and analyzed for evaluating the performance of the proposed model. The analysis proves the effectiveness and practicality of the proposed model is participation of VPP in electricity markets. © 2018 Journal of Energy Management and Technology

**keywords:** Virtual power plant, combined heat and power, NaS battery storage, power market, distributed generation.

<http://dx.doi.org/10.22109/jemt.2018.133447.1095>

## 1. INTRODUCTION

The penetration of renewable energy sources containing wind turbines and photovoltaic systems have been increased in power systems according to significant advantages of such power sources, which include reduction of pollutant gas emission, decrement of power losses, improving power quality and reliability indexes of the system, peak shaving and voltage regulation [1, 2]. On the other hand, micro generation units such as combined heat and power (CHP) units and diesel generators have been integrated to power systems in order to attain active distribution networks and overcome issues appeared by dramatic increment of load and insufficient power sources [3]. Micro generation units are not capable to participate in power market, which has been proceeded by appearing concept of virtual power plants (VPPs). The main objective of VPP concept is managing a vast group of micro generation units, whose total capacity can be considered as a conventional power unit. All kinds of micro generation units can be considered in VPP concept including renewable energy sources, conventional power units, battery storage units, and controllable loads. VPPs permits the small generation units to assess the power market in aggregated

form. In addition, such units compensate unexpected power fluctuations of renewable energy sources [4, 5].

Energy storage units are introduced as practical solution to overcome fluctuations associated with power generation output of renewable energy sources, which are important technologies of smart grids. The application of energy storage units takes advantages of providing ancillary services, improving reliability indexes of the system, and peak load shaving [6]. The energy storage units and application of such units in energy systems have been investigated in the area of power system planning [7], energy markets [8], joint energy and reserve markets [9], and operation of micro-grids [10]. Different technologies have been introduced for storing energy in power network including compressed air energy storage (CAES) [11], pumped-storage units [12], spinning reserve criterion [13], fuel-cell technology [14], NaS storage [15], superconducting storage [16] and lithium-ion batteries [17]. The authors have studied the application of fuel cell and electrical energy storage systems in optimal scheduling of a fuel cell-CHP based micro-grids in [3], where the micro-grid is able to store the energy as electrical energy/hydrogen in off-peak hours and use it in on-peak hours.

In [12], a coordinated scheduling framework is proposed for unit commitment of a wind-pumped storage integrated system. The effect of CAES unit in stochastic unit commitment problem of a power system is investigated in [11] considering static voltage stability analysis.

CHP plants produce heat and power, simultaneously by recovering the wasted heat during production process of power by conventional thermal units [18]. The implementation of CHP unit takes advantages of increasing the efficiency of providing power and heat demands as 90% and reducing emission of pollutant gases almost 13-18% [19, 20]. The optimal power and heat production scheduling of CHP plants should be provided satisfying mutual dependency of generated power and heat of such units, which is known as feasible operating region. Various methods have been implemented for handling the optimal scheduling of the CHP units and dealing with feasible operating regions of such units such as Lagrangian relaxation [21], benders decomposition [22], mixed integer non-linear programming [23] and branch and bound method [24]. A robust model is proposed in [10] for studying the uncertainty of power market price in optimal scheduling of integrated heat and power micro-grids to attain the optimal operation cost of the micro-grid in worst-case condition of the power market price. In [25], real coded genetic algorithm with improved Mühlenbein mutation is proposed for obtaining optimal economic dispatch of CHP units in order to satisfy the heat and power loads considering the operational and electrical constraints. The authors have studied optimal scheduling of CHP units in the day-ahead wholesale energy markets using mixed-integer nonlinear programming in [23] considering nonlinear dynamics of a CHP unit and the related individual components.

The main objective of this study is investigating optimal scheduling of VPP including NaS battery storage, CHP units, and wind turbine as renewable energy source. The VPP studied in this paper not only is able to cooperate in power market, but also, is capable to supply heat demand of adjacent area. The proposed model is simulated and the results are provided and analyzed, which shows the effectiveness and practicality of the model.

This paper is organized as follows: Section 2 prepares the problem formulation of optimal scheduling VPPs. Case study and simulation results are provided in Section 3. Finally, the conclusion of paper is accomplished Section 4

## 2. PROBLEM FORMULATION

The mathematical model of VPP plant and distinct heat are investigated in this section. The VPP includes micro generators, CHP units and NaS batteries as electrical equipment. Also, CHP units, boiler, and thermal storage are installed for supplying heat demand. The mathematical of each components are introduced in the following.

### A. CHP units

The operational cost of CHP units is modeled in (1). According this model can conclude that CHP cost depends on heat and power generated in each time.

$$C_j(t, s) = a_j(P_j(t, s))^2 + b_j P_j(t, s) + c_j + d_j(H_j(t, s))^2 + e_j H_j(t, s) + f_j H_j(t, s) P_j(t, s) \quad (1)$$

where, the parameters  $a_j$ ,  $b_j$ ,  $c_j$ ,  $d_j$ ,  $e_j$  and  $f_j$  show the cost coefficients of the  $j^{\text{th}}$  CHP plant. The power and heat generated by  $j^{\text{th}}$

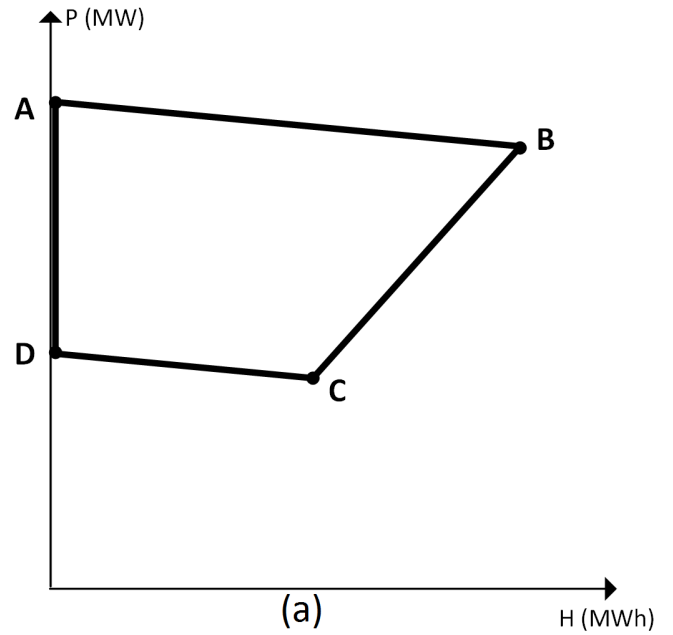


Fig. 1. FOR of CHP type 1

CHP plant in  $s^{\text{th}}$  scenario are determined by  $P_j(t, s)$ ,  $H_j(t, s)$ , respectively. Total CHP cost for time  $t$  in  $s^{\text{th}}$  scenario is illustrated by  $C_j(t, s)$ . Also, the heat and power produced by CHP unit are limited to its minimum and maximum values. This constraint is show in (2).

$$\begin{aligned} P_j^{c_{\min}} \times V_j(t, s) &\leq P_j(t, s) \leq P_j^{c_{\max}} \times V_j(t, s) \\ H_j^{c_{\min}} \times V_j(t, s) &\leq H_j(t, s) \leq H_j^{c_{\max}} \times V_j(t, s) \end{aligned} \quad (2)$$

where, the lower and upper bounds of power generation of  $j^{\text{th}}$  CHP plant are defined by  $P_j^{c_{\min}}$  and  $P_j^{c_{\max}}$ , respectively. In addition, the respective indicators for minimum and maximum heat generation of  $j^{\text{th}}$  CHP plant are defined by  $H_j^{c_{\min}}$  and  $H_j^{c_{\max}}$ , respectively. The binary variable  $V_j(t, s)$  is used to define the ON/OFF status of the  $j^{\text{th}}$  CHP plant in  $s^{\text{th}}$  scenario.

Fig. 1 shows the feasible operating region (FOR) for CHP type 1. The feasible operating region of the CHP type-1 can be stated as equations (3)-(7).

$$\begin{aligned} P_{CHP1}(t, s) - P_{CHP1}(A, s) - \frac{P_{CHP1}(A, s) - P_{CHP1}(B, s)}{H_{CHP1}(A, s) - H_{CHP1}(B, s)} \\ \times (H_{CHP1}^t(t, s) - H_{CHP1}(A, s)) \leq 0 \end{aligned} \quad (3)$$

$$\begin{aligned} P_{CHP1}(t, s) - P_{CHP1}(B, s) - \frac{P_{CHP1}(B, s) - P_{CHP1}(C, s)}{H_{CHP1}(B, s) - H_{CHP1}(C, s)} \\ \times (H_{CHP1}(t, s) - H_{CHP1}(B, s)) \geq -(1 - V_{CHP1}(t, s)) \times M \end{aligned} \quad (4)$$

$$\begin{aligned} P_{CHP1}(t, s) - P_{CHP1}(C, s) - \frac{P_{CHP1}(C, s) - P_{CHP1}(D, s)}{H_{CHP1}(C, s) - H_{CHP1}(D, s)} \\ \times (H_{CHP1}(t, s) - H_{CHP1}(C, s)) \geq -(1 - V_{CHP1}(t, s)) \times M \end{aligned} \quad (5)$$

Equations (3) and (4) define the area under the curve AB, and under the curve BC. In addition, equation (5) shows the area under the curve CD. FOR of CHP type 2 is demonstrated in Fig. 2. CHP type 2 has a non-convex characteristic, which is divided

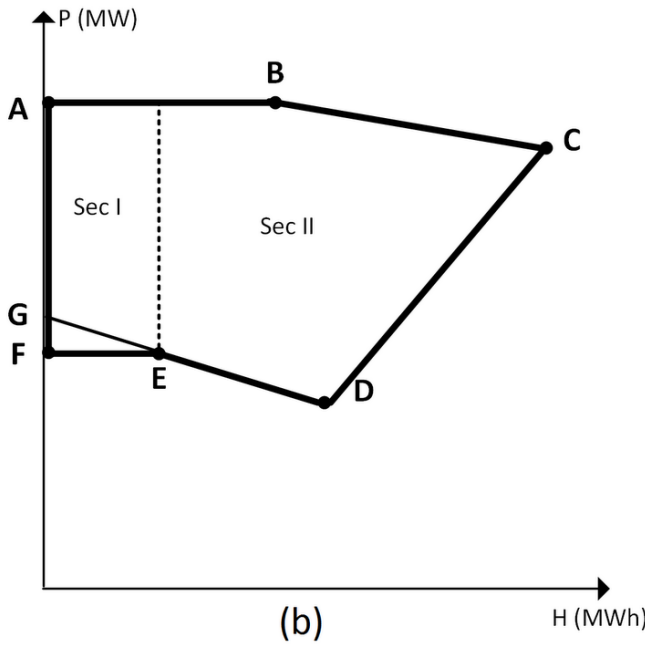


Fig. 2. FOR of CHP type 2

to two convex regions. Equations (6)-(12) are applied to model the FOR region.

$$P_{CHP2}(t,s) - P_{CHP2}(B,s) - \frac{P_{CHP2}(B,s) - P_{CHP2}(C,s)}{H_{CHP2}(B,s) - H_{CHP2}(C,s)} \times (P_{CHP2}(t,s) - P_{CHP2}^B(B,s)) \leq 0 \quad (6)$$

$$P_{CHP2}(t,s) - P_{CHP2}(C,s) - \frac{P_{CHP2}(C,s) - P_{CHP2}(D,s)}{H_{CHP2}(C,s) - H_{CHP2}(D,s)} \times (H_{CHP2}(t,s) - H_{CHP2}(C,s)) \geq 0 \quad (7)$$

$$P_{CHP2}(t,s) - P_{CHP2}(E,s) - \frac{P_{CHP2}(E,s) - P_{CHP2}(F,s)}{H_{CHP2}(E,s) - H_{CHP2}(F,s)} \times (H_{CHP2}(t,s) - H_{CHP2}(E,s)) \geq -(1 - X_1(t,s)) \times M \quad (8)$$

$$P_{CHP2}(t,s) - P_{CHP2}(D,s) - \frac{P_{CHP2}(D,s) - P_{CHP2}(E,s)}{H_{CHP2}^D(t,s) - H_{CHP2}^E(t,s)} \times (H_{CHP2}(t,s) - H_{CHP2}(D,s)) \geq -(1 - X_2(t,s)) \times M \quad (9)$$

$$X_1(t,s) + X_2(t,s) = V_{CHP2}(t,s) \quad (10)$$

$$H_{CHP2}(t,s) - H_{CHP2}(E,s) \leq (1 - X_1(t,s)) \times M \quad (11)$$

$$H_{CHP2}(t,s) - H_{CHP2}(E,s) \geq -(1 - X_2(t,s)) \times M \quad (12)$$

Equations (6) and (7) define the under the curve BC, and upper the curve CD. In addition, the upper areas of curves EF and DE are defined by (8) and (9).

### B. Wind turbine

Due to the low operation cost of wind power generation, operational cost of such plants is often neglected in research studies. The total power of wind farm is modeled as follow:

$$P_W(k,t,s) = \begin{cases} 0 & V_{WS}(t,s) \leq V_{cutin}(k), V_{WS}(t,s) \geq V_{cutout}(k) \\ P_{WG\max}(k) \times \left( \frac{V_{WS}(t,s) - V_{cutin}(k)}{V_{rated}(k) - V_{cutin}(k)} \right)^3 & V_{cutin}(k) \leq V_{WS}(t,s) \leq V_{rated}(k) \\ P_{WG\max}(k) & V_{rated}(k) \leq V_{WS}(t,s) \leq V_{cutout}(k) \end{cases} \quad (13)$$

Wind speed and wind turbine characteristics are two parameters which are utilized to model power injection of wind plants. The

available power of  $k$ th wind turbine at time  $t$  in  $s^{th}$  scenario is indicated by  $P_W(k,t,s)$ . The cut-in, cut-out and rated speed of the wind turbine  $k$  are defined by  $V_{cutin}(k)$ ,  $V_{cutout}(k)$  and  $V_{rated}(k)$ . The nominal power output of the  $k^{th}$  wind turbine is determined by  $P_{WG\max}(k)$ .

### C. NaS

Sodium sulfur (NaS) batteries are generally installed in wide range of power ratings from 1.0 MW to 34 MW. This storage can operate in three mode (charging, discharging, and off line) equal other storage. A NaS batteries can formulated as follow:

$$u_s(t,s) \leq N_{pulse}(t,s) \leq 2.6u_s(t,s) \quad (14)$$

$$0 \leq P_s(t,s) \leq N_{pulse}(t,s)P_{\max} \quad (15)$$

$$0 \leq P_p(t,s) \leq u_p(t,s)P_{\max} \quad (16)$$

$$u_s(t,s) + u_p(t,s) \leq 1 \quad (17)$$

$$E(t,s) = E(t-1) - E_p(t,s) + \eta E_s(t,s) - P_{loss}(t,s) \quad (18)$$

$$E_{\min} \leq E(t,s) \leq E_{\max} \quad (19)$$

$$d(t,s) = 3.4497N_{pulse}^3(t,s) + 21.5962N_{pulse}^2(t,s) \quad (20)$$

$$-45.7961N_{pulse}(t,s) + 34.7117$$

$$P_{loss}(t,s) = \frac{7 - (N_{pulse}(t,s) \times d(t,s))}{d(t,s)} u(t,s) \quad (21)$$

The constraint (14) is used to model NaS pulse limitation. In this equation, the pulse number is demonstrated by  $N_{pulse}$ . In addition, the binary variable  $u_s$  is used to determine charging mode. The active and reactive power outputs through the AC-DC converter can be controlled independently by NaS battery. The power can be instantaneously discharged by such system from one to five times as much as the rated capacity by sufficient capacity of the AC-DC converter device. NaS battery has a limitation of output based on the internal temperature. Due to participation VPP in day ahead market, the maximum value of  $N_{pulse}$  is set as 2.6. The power charging and discharging of the NaS battery at time  $t$  in scenario  $s$  are defined by  $P_s(t,s)$  and  $P_p(t,s)$ . The lower and upper limitation of charging and discharging ( $P_{\max}$ ) modes are considered in (15), (16), respectively. The storage can operate as a certain mode each period. The constraint (17) satisfies this limitation. The energy balance is formulated in (18). In this constraint,  $E$  is the energy stored in battery and  $P_{loss}$  is the battery loss, which is calculated by using (20), (21). The minimum ( $E_{\min}$ ) and maximum ( $E_{\max}$ ) limits of energy stored amount are provided by (19). In (20), the NaS pulse trend is modeled by a third order polynomial. In addition, the power loss versus different NaS pulse factors is obtained by (21).

### D. Boiler

The operation cost of the boiler is a function of generated heat by such units, which can be stated as:

$$C(H_b^t) = \lambda_b \times H_b^t \quad (22)$$

The heat generated by boiler should be limited to its lower and upper bounds as:

$$H_b^{\min} \times V_b^t \leq H_b^t \leq H_b^{\max} \times V_b^t \quad (23)$$

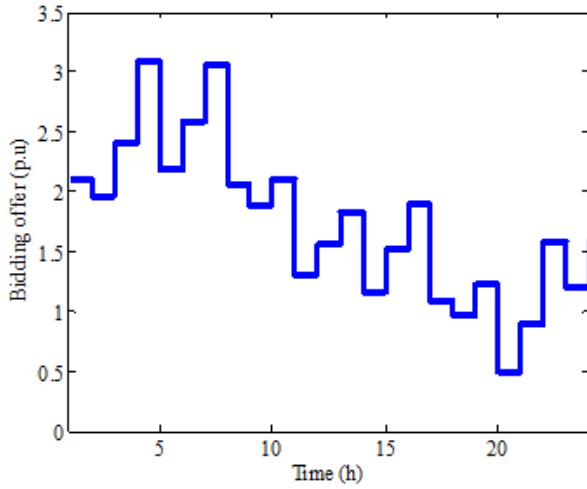


Fig. 3. Bidding offer of the VPP

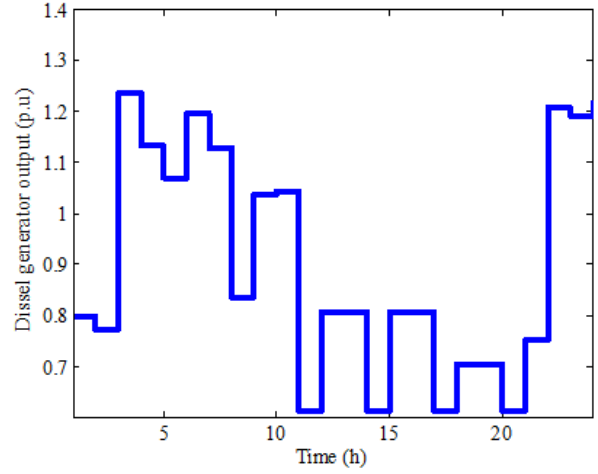


Fig. 4. Total power output of CHP units

**E. Thermal Storage**

The thermal storage is modelled as following:

$$H_{ch}^{min} \times V_s^t \leq H_{ch}^t \leq H_{ch}^{max} \times V_{ch}^t \quad (24)$$

$$H_{disch}^{min} \times U_{disch}^t \leq H_{disch}^t \leq H_{disch}^{max} \times U_{disch}^t \quad (25)$$

$$U_{ch}^t + U_{disch}^t \leq 1 \quad (26)$$

$$A_h^{t+1} = A_h^t + H_{ch}^t - H_{disch}^t \quad (27)$$

The minimum and maximum limitation of charging mode of heat storage are accounted by (24). The similar limitations for discharge condition are provided in (25). The operation of storage in one of the charge/discharge/ideal modes is considered in (26). The heat balance of thermal storage is studied by (27).

**F. Objective function**

The objective function of VPP include the operational cost of CHP plants, the boiler cost and diesel generator operation cost, which can be stated as follows:

$$\max \sum_{t=1}^{24} \sum_{s=1}^{S_n} \pi_s \lambda_s^t P_D^t - \sum_{s=1}^{S_n} \pi_s (C_{CHP} + C_{boiler} + C_{diesel}) \quad (28)$$

**3. CASE STUDY AND SIMULATION RESULTS**

The studied VPP includes wind turbine, two types of CHP units, NaS battery storage system, thermal storage unit and boiler. The proposed model is solved as mixed integer non-linear programming (MINLP) [26] under General Algebraic Modeling System (GAMS) environment [27]. The expected bidding offer of the VPP during the scheduling time horizon is proposed in Fig. 3. As seen in this figure, the maximum bidding offer of the VPP is related to  $t=4$  h, where the bidding offer is equal to 3.14 p.u., and the minimum bidding offer is related to  $t = 20$ , where the bidding offer is equal to 0.48 p.u.

Total power output of CHP units in p.u. is shown in Fig. 4. As it is obvious from this figure, total power generation of CHP plants at  $t = 3, 6, 23,$  and  $24$  h are more than other hours. The CHP units have participated in supplying power demand during the whole scheduling time interval. Power discharge

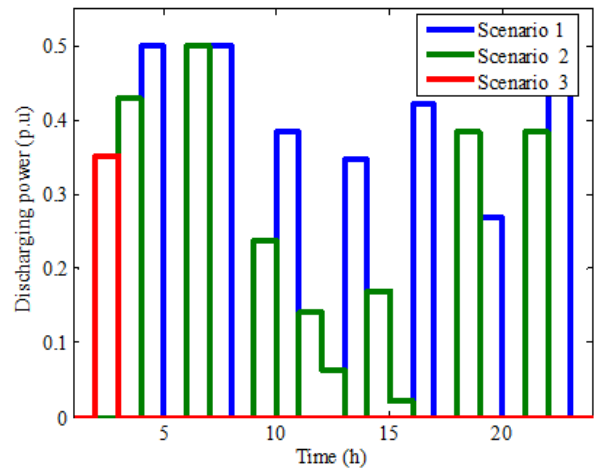


Fig. 5. Power discharge of the NaS battery

of the NaS battery is depicted for the scheduling time horizon for three scenarios in Fig. 5. The results are reported for three different scenarios. Power charge of the NaS battery is shown for the scheduling time interval for three scenarios in Fig. 6. Similar to power charge of the NaS battery, the results are reported for three scenarios. Considering Figs.5 and 6, the NaS battery has operated only in one of the charge/discharge/idle mode at each time in each of the three studied scenarios. The sum of power generation by two CHP units and power discharge of the Nas batter minus the power charge of the Nas battery storage unit has satisfied the power load demand at each time.

The sum of heat generation by two types of CHP plants are shown in Fig. 7. As it is obvious, the CHP units have participated in heat supply of the system with respect to boiler due to low generation cost of the CHP units. Figure 8 Shows the boiler heat output, which have generated heat at  $t = 1$  and time interval between  $t = 11$  h and  $t = 22$  h. The boiler has not participated in supplying heat demand between  $t = 4$  h and  $t = 11$  h due to lower generation cost of the CHP units at this time interval. The sum of heat generated by CHP units and the boiler has satisfied the heat demand during the scheduling time interval. Figure 9

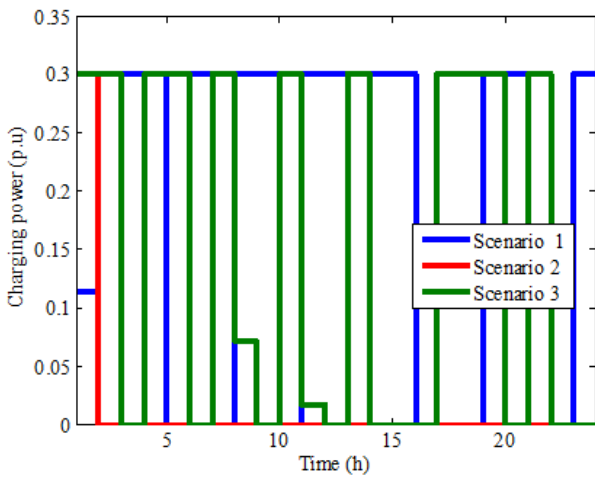


Fig. 6. Power charge of the NaS battery

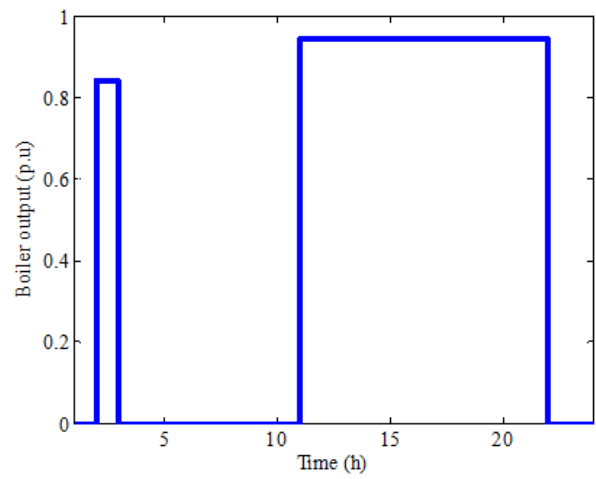


Fig. 8. Boiler heat output

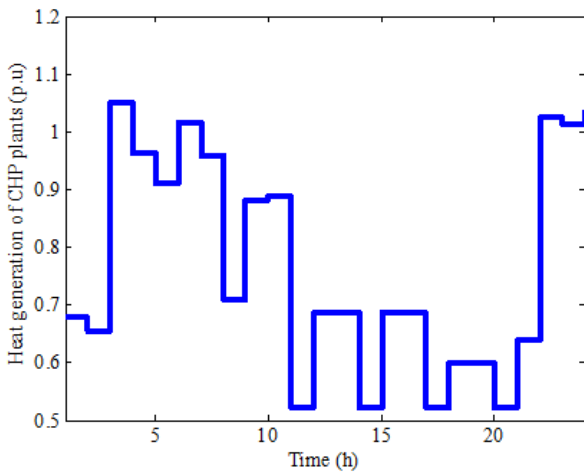


Fig. 7. Total heat generation by CHP units

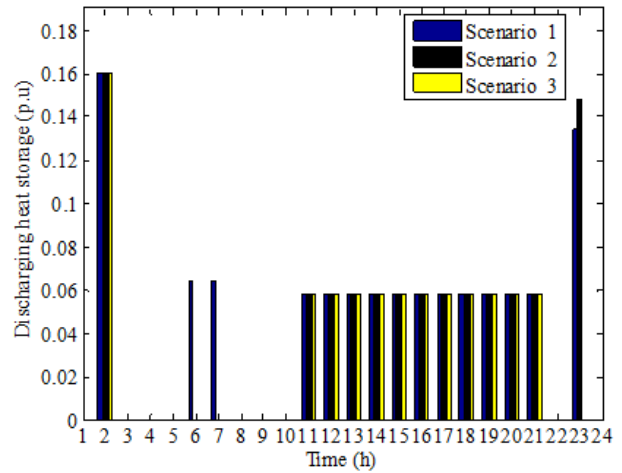


Fig. 9. Heat discharge of the thermal storage unit

shows the heat discharge of the thermal storage unit for three scenarios. Heat charge of the thermal storage unit is shown in Fig. 10. The results are provided for three scenarios, which shows that the heat charge of thermal storage in scenario 1 is more than other scenarios.

**4. CONCLUSION**

In this paper, a stochastic model is proposed for optimal scheduling of virtual power plants, which integrates small-scale distributed generations and renewable power units and investigates the participation of such units into power markets. The proposed model is studied for a system including distributed generations, renewable power units, two different kinds of combined heat and power (CHP), boiler, NaS battery and thermal storage unit. The proposed model studies the participation of VPP into day-ahead market supplying local heat demand. The stochastic model is accounted for scheduling of VPP to study the uncertainties associated with wind power generation outputs. The simulation results of the proposed stochastic model are reported for a case study and are analyzed in order to evaluate the performance of the proposed model. The simulation results

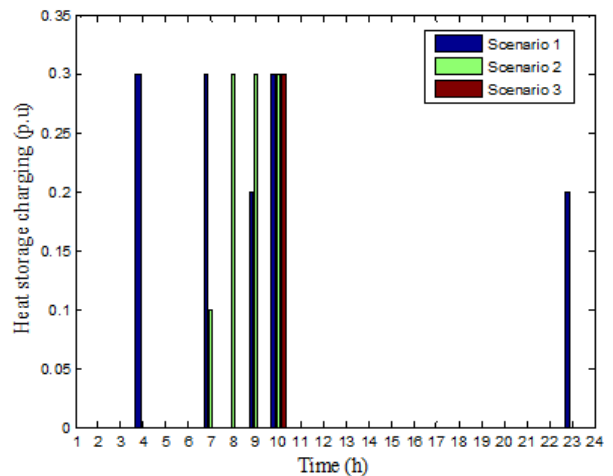


Fig. 10. Heat charge of the thermal storage unit

show the successful participation of VPP and NaS battery storage in electricity markets to meet the power load demand and satisfy the head load demand of the system.

## REFERENCES

1. Sedghi, Mahdi, Ali Ahmadian, and Masoud Aliakbar-Golkar. "Optimal storage planning in active distribution network considering uncertainty of wind power distributed generation." *IEEE Transactions on Power Systems* 31, no. 1 (2016): 304-316.
2. Naderi, Ehsan, Hossein Seifi, and Mohammad Sadegh Sepasian. "A dynamic approach for distribution system planning considering distributed generation." *IEEE Transactions on Power Delivery* 27, no. 3 (2012): 1313-1322.
3. Nazari-Heris, Morteza, Saeed Abapour, and Behnam Mohammadi-Ivatloo. "Optimal economic dispatch of FC-CHP based heat and power micro-grids." *Applied Thermal Engineering* 114 (2017): 756-769.
4. Giuntoli, Marco, and Davide Poli. "Optimized thermal and electrical scheduling of a large scale virtual power plant in the presence of energy storages." *IEEE Transactions on Smart Grid* 4, no. 2 (2013): 942-955.
5. Houwing, Michiel, Georgios Papaefthymiou, Petra W. Heijnen, and Marija D. Ilic. "Balancing wind power with virtual power plants of micro-CHPs." In *PowerTech, 2009 IEEE Bucharest*, pp. 1-7. IEEE, 2009.
6. Awad, Ahmed SA, J. David Fuller, Tarek HM El-Fouly, and Magdy MA Salama. "Impact of energy storage systems on electricity market equilibrium." *IEEE Transactions on Sustainable Energy* 5, no. 3 (2014): 875-885.
7. Bustos, Carlos, E. Sauma, Sebastian de la Torre, José Aguado, Javier Contreras, and David Pozo. "Energy storage and transmission expansion planning: substitutes or complements?." *IET Generation, Transmission Distribution*(2017).
8. Mohsenian-Rad H. Coordinated price-maker operation of large energy storage units in nodal energy markets. *IEEE Transactions on Power Systems*. 2016;31:786-97.
9. Eichman J, Denholm P, Jorgenson J, Helman U. Operational Benefits of Meeting California's Energy Storage Targets. NREL (National Renewable Energy Laboratory (NREL), Golden, CO (United States)); 2015.
10. Nazari-Heris, M., Mohammadi-Ivatloo, B., Gharehpetian, G. B., Shahidehpour, M. (2018). Robust Short-Term Scheduling of Integrated Heat and Power Microgrids. *IEEE Systems Journal*, (99), 1-9.
11. Ghaljehei, M., Ahmadian, A., Golkar, M. A., Amraee, T., Elkamel, A. (2018). Stochastic SCUC considering compressed air energy storage and wind power generation: A techno-economic approach with static voltage stability analysis. *International Journal of Electrical Power Energy Systems*, 100, 489-507.
12. Jiang, R., Wang, J., Guan, Y. (2012). Robust unit commitment with wind power and pumped storage hydro. *IEEE Transactions on Power Systems*, 27(2), 800.
13. Pavić, I., Capuder, T., Kuzle, I. (2015). Value of flexible electric vehicles in providing spinning reserve services. *Applied Energy*, 157, 60-74.
14. Mahato, N., Banerjee, A., Gupta, A., Omar, S., Balani, K. (2015). Progress in material selection for solid oxide fuel cell technology: A review. *Progress in Materials Science*, 72, 141-337.
15. Haessig, P., Multon, B., Ahmed, H. B., Lascaud, S., Jamy, L. (2013, June). Aging-aware NaS battery model in a stochastic wind-storage simulation framework. In *PowerTech (POWERTECH), 2013 IEEE Grenoble* (pp. 1-6). IEEE.
16. Abraham, R. J., Thomas, A. (2016). A Genetic Proportional Integral Derivative Controlled Hydrothermal Automatic Generation Control with Superconducting Magnetic Energy Storage. In *Electricity Distribution* (pp. 267-284). Springer, Berlin, Heidelberg.
17. Choi, J. W., Aurbach, D. (2016). Promise and reality of post-lithium-ion batteries with high energy densities. *Nature Reviews Materials*, 1(4), 16013.
18. Nazari-Heris M, Mehdinejad M, Mohammadi-Ivatloo B, Babamalek-Gharehpetian G. Combined heat and power economic dispatch problem solution by implementation of whale optimization method. *Neural Computing and Applications*.1-16.
19. Nazari-Heris M, Mohammadi-Ivatloo B, Gharehpetian G. A comprehensive review of heuristic optimization algorithms for optimal combined heat and power dispatch from economic and environmental perspectives. *Renewable and Sustainable Energy Reviews*. 2017.
20. Vasebi A, Fesanghary M, Bathaee S. Combined heat and power economic dispatch by harmony search algorithm. *International Journal of Electrical Power Energy Systems*. 2007;29:713-9.
21. Sashirekha A, Pasupuleti J, Moin N, Tan C. Combined heat and power (CHP) economic dispatch solved using Lagrangian relaxation with surrogate subgradient multiplier updates. *International Journal of Electrical Power Energy Systems*. 2013;44:421-30.
22. Abdolmohammadi HR, Kazemi A. A benders decomposition approach for a combined heat and power economic dispatch. *Energy conversion and management*. 2013;71:21-31.
23. Kim JS, Edgar TF. Optimal scheduling of combined heat and power plants using mixed-integer nonlinear programming. *Energy*. 2014;77:675-90.
24. Rong A, Lahdelma R. An efficient envelope-based Branch and Bound algorithm for non-convex combined heat and power production planning. *European Journal of Operational Research*. 2007;183:412-31.
25. Haghrah, A., Nazari-Heris, M., Mohammadi-Ivatloo, B. (2016). Solving combined heat and power economic dispatch problem using real coded genetic algorithm with improved Mühlenbein mutation. *Applied Thermal Engineering*, 99, 465-475.

26. R. E. Rosenthal GusgaeW, DC UGdc, 2012 [Online]. Available; <http://www.gams.com/dd/docs/solvers/conopt.pdf>.
27. A. Brooke DK, and A. Meeraus. (1990). Gams User's Guide, <http://www.gams.com/docs/gams/GAMSUsersOA,Guide.pdf>.